IEEE Access
Multidisciplinary | Rapid Review | Open Access Journal

Received January 23, 2019, accepted February 22, 2019, date of current version March 25, 2019.

Digital Object Identifier 10.1109/ACCESS.2019.2901799

Enhancement of Strain/Temperature Measurement Range and Spatial Resolution in Brillouin Optical Correlation Domain Analysis Based on Convexity Extraction Algorithm

BIN WANG, XINYU FAN, (Senior Member, IEEE), YUANXIU FU, AND ZUYUAN HE, (Senior Member, IEEE)

Shanghai Institute for Advanced Communication and Data Science, State Key Laboratory of Advanced Optical Communication Systems and Networks, Department of Electronic Engineering, Shanghai Jiao Tong University, Shanghai 200240, China

Corresponding author: Xinyu Fan (fan.xinyu@sjtu.edu.cn)

This work was supported in part by the National Natural Science Foundation of China (NSFC) under Grant 61775132, Grant 61735015, and Grant 61620106015, and in part by the State Grid Corporation of China under Grant 5455HT170031.

ABSTRACT We propose and experimentally demonstrate a novel method to enhance the performance of the Brillouin optical correlation domain analysis (BOCDA) by analyzing the shape characteristic of the measured Brillouin gain spectrum. We theoretically analyze and simulate the operation of BOCDA, and it is found that the Brillouin signal peak generated at the correlation peak shows a sharp Lorentzian shape with a large value of convexity, while the background noise structure stacked from other positions shows a smooth trapezoidal shape with a small value of convexity. By extracting the convexity of measured BGS, the signal part can be enhanced while the noise part is suppressed drastically, which leads to an enlarged strain/temperature measurement range and a narrowed spatial resolution for BOCDA. This concept is verified by both numerical simulation and experiments. By using this method, a $>$16-mε/800-°C strain/temperature measurement range and a fivefold-improved spatial resolution are achieved experimentally without extra hardware complexity.

INDEX TERMS Brillouin scattering, BOCDA, optical fiber sensors, temperature sensors, strain measurement, spatial resolution.

I. INTRODUCTION

Distributed fiber sensors based on Brillouin scattering have been regarded as a powerful tool for temperature or strain measurement in health monitoring of various structures due to their capability to provide continuous information along the whole fiber used for sensing. To date, various schemes of distributed Brillouin sensors have been successfully developed in the domain of time [1], frequency [2], and correlation [3]. Among them, Brillouin sensors based on time-domain operation provide the advantage of long measurement range up to 100 km [4]–[7]. However, the spatial resolution of conventional Brillouin time-domain sensors is limited to several meters, which is determined by the width of the optical pulse launched into the fiber under test (FUT). Recently, several modified Brillouin time-domain sensors with high spatial resolution have been proposed, such as differential pulse-width pair (DPP) scheme [8]–[10], Brillouin echoes scheme [11], [12], and dark-pulse scheme [13]. In these schemes, the spatial resolution is determined by the differential width of the optical pulse pair, and a centimeter-level spatial resolution can be realized. However, one major drawback is that an ultrahigh-bandwidth receiver module is required to achieve a high spatial resolution (for example, a $>$5-GHz receiving bandwidth is required for a 2-cm spatial resolution), which greatly increases the cost of these sensing systems, restricting their applications in practical environment.

On the contrary, Brillouin correlation-domain sensors provide ultrahigh spatial resolution intrinsically. In a correlation-domain sensing system, correlation peaks are normally synthesized to generate position-dependent Brillouin interaction, so as to implement distributed measurement.

The associate editor coordinating the review of this manuscript and approving it for publication was Kin Kee Chow.

Up to now, various Brillouin correlation-domain sensing schemes have been developed. For example, Brillouin optical correlation domain analysis (BOCDA) based on pseudo-random binary sequence (PRBS) phase modulation has been proposed, which are capable of achieving a large number of effective sensing points [14], [15]. However, in this scheme, a costly PRBS generator with a large bandwidth (∼5 GHz) is required to realize a high spatial resolution. Alternately, BOCDA systems based on amplified spontaneous emission (ASE) source or chaotic laser are able to provide a high spatial resolution in a much simpler way [16]–[19], but the signal-to-noise (SNR) is very poor, leading to a deteriorated measurement accuracy. Moreover, the scanning of the correlation peak in this scheme is realized by using a mechanical variable delay line, thus the speed of distributed measurement is very slow.

As another successful method, Brillouin correlation-domain sensors based on sinusoidal frequency modulation are able to simultaneously provide high spatial resolution, high measurement accuracy, high measurement speed, and low complexity [3], [20]–[26]. In this scheme, both the pump lightwave and the probe lightwave are sinusoidally modulated to synthesize periodical correlation peaks along the FUT. The measurement range and the spatial resolution are determined by the interval and the full width at half maximum (FWHM) of the correlation peaks. Although this BOCDA system provides impressive performance, there is a trade-off relation between the measurement range and the spatial resolution, leading to a limited number (∼1000) of effective sensing points. In order to solve this problem, several performance-enhancing techniques have been proposed, including the temporal-gating scheme [27], dual-frequency modulation scheme [28], and bidirectional measurement scheme [29]. Although existing techniques have made important progresses, actually, none of them take full advantage of all information contained in the measured data, which gives room for substantial improvement by utilizing post-data processing technique.

In this paper, we newly propose a method to enhance the performance of BOCDA by extracting the convexity of the measured Brillouin gain spectrum (BGS). In BOCDA, the measured BGS is composed of the Lorentzian-shape Brillouin signal generated at the correlation peak and a trapezoidal noise structure accumulated from all other positions along the FUT. When the temperature is increased or a strain is applied to the FUT, the Brillouin signal will shift to a higher frequency, while the trapezoidal noise structure remains unchanged. Normally, the Brillouin frequency shift (BFS) is obtained by searching for the frequency corresponding to the maximum Brillouin gain. When the noise level becomes higher than the Brillouin signal, the detection will fail and the strain/temperature information cannot be measured correctly. Several techniques including intensity modulation (IM) and differential detection scheme have been proposed to solve this problem [30], [31], but with extra hardware complexity, and rigid synchronization is required to ensure stable operation. Here, to suppress the background noise, we extract the convexity of the measured BGS. According to the theoretical analysis, the sharp (Lorentzian-shape) Brillouin signal from the correlation peak shows a large value of convexity, while the smooth trapezoidal noise structure shows a small value of convexity. In this case, when the convexity extraction algorithm is introduced, the Brillouin signal from the correlation peak is improved, while the trapezoidal noise accumulated from other positions is suppressed drastically, leading to a larger strain/temperature measurement range and a higher spatial resolution. The feasibility of the proposed method is verified by both numerical simulation and experiments. The strain/temperature measurement range of BOCDA is enlarged from ∼240 MHz (∼4.8 mε/240 °C) to >800 MHz (>16 mε/800 °C) when the convexity is utilized to measure the BFS. When distributed measurements are implemented, the spatial resolution is improved from 40 cm to 8 cm for a measurement range of ∼700 m, or from 2 cm to 4 mm for a measurement range of ∼20 m, showing a fivefold enhancement of spatial resolution. It is desired to mention that all these enhancements are obtained without extra hardware complexity.

II. THEORETICAL ANALYSIS AND NUMERICAL SIMULATION

In the BOCDA system, the pump and the probe are jointly sinusoidally-modulated to synthesize periodical correlation peaks. By scanning the correlation peak along the whole FUT, distributed measurements of strain/temperature can be implemented. The modulation frequency and amplitude are expressed as f_m and Δf, respectively. The pump and the probe are counter-propagating in the FUT, and the generated beat frequency signal $f_{beat}(t)$ is given as

$$f_{beat}(t) = v_B + \Delta f\,[\sin(2\pi f_m t) - \sin(2\pi f_m (t-\tau))] \quad (1)$$

where v_B is the BFS of the FUT and τ is the time delay between the pump and the probe, which can be given as $2x/v_g$, where x is the longitudinal distance between the pump and the probe, and v_g is the group velocity of light in fiber. The power spectrum of the beat frequency signal can be expressed as the function of the distance x and the pump-probe frequency difference f, as [32]

$$\begin{cases} S_b(x, \pm kf_m) = \left|J_k(4\pi\,\Delta f x/V_g)\right|^2 & (f = \pm kf_m) \\ S_b(x, f) = 0 & (f \neq \pm kf_m) \end{cases} \quad (2)$$

where J_k are k-th order Bessel functions of the first kind. The local BGS of the FUT shows a Lorentzian shape, which can be formulated as [33]

$$G(x, f) = \frac{g_0}{1 + 4(f - v_B(x))/\Delta v^2} \quad (3)$$

where g_0 is the Brillouin gain coefficient, $v_B(x)$ is the BFS at position x, and Δv is the Brillouin gain linewidth (∼35 MHz). Then, the BGS distribution measured by BOCDA can be calculated as the 2-dimensional convolution

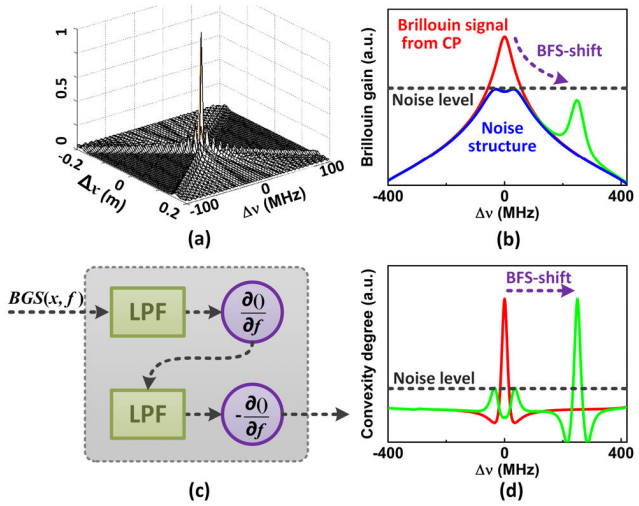

FIGURE 1. (a) Simulation result of the beat spectrum when the modulation frequency f_m and amplitude Δf are set to be 2.1 MHz and 5.1 GHz. (b) The Brillouin gain spectrum (BGS) obtained by BOCDA, which consists of not only the Brillouin signal from the correlation peak but also the noise structure accumulated from other positions along the fiber under test (FUT). (c) The schematic diagram of convexity extraction algorithm. (d) The extracted convexity of the BGS, showing a suppression of the background noise structure.

of the beat spectrum $S_b(x,f)$ and the local BGS $G(x,f)$ [32], as

$$BGS(x,f)=\frac{v_g P}{A_{eff}}\int_{f_0}\int_{x_0} G(x_0,f_0)S_b(x_0-x,f_0-f)dx_0\ df_0 \tag{4}$$

where P is the time-averaged pump power and A_{eff} is the effective core area of the fiber.

Figure 1(a) shows the numerical simulation of the beat spectrum $S_b(x,f)$ when the modulation frequency f_m and the modulation amplitude Δf are set to be 2.1 MHz and 5.1 GHz, respectively. It is clear that the beat spectrum becomes a sharp δ-function at the correlation peak, while spreads widely at other positions. Thus, after calculating convolution with the local BGS, the Brillouin signal generated from the correlation peak remains a sharp Lorentzian shape, as shown in Fig. 1(b) (red line). In the BGS measured by BOCDA, besides the Brillouin signal from the correlation peak, a trapezoidal noise structure (blue line in Fig. 1(b)) which is stacked from all other positions along the FUT can also be observed. When a strain is applied to the FUT, the Brillouin signal generated from the correlation peak will shift to a higher frequency, while the noise structure remains unchanged. When the BFS shift is larger than the strain/temperature measurement range (~240 MHz, or 4.8 mε/240 °C) of BOCDA or the stretched length is shorter than the nominal spatial resolution, the noise level may become higher than the Brillouin signal from the correlation peak, as shown in Fig. 1(b) (green line). In this case, the BFS cannot be obtained correctly with the conventional method which searches for the frequency corresponding to maximum Brillouin gain, even though the useful Brillouin signal is contained in the measured BGS.

To magnify the Brillouin signal from the correlation peak and suppress the background noise, a convexity extraction algorithm is proposed. It is clear that the Brillouin signal from the correlation peak shows a sharp Lorentzian shape, thus having a large value of convexity, while the background noise shows a trapezoidal shape, thus having a small value of convexity. Therefore, when the convexity is utilized to determine the BFS, the background noise can be suppressed drastically. Fig. 1(c) depicts the schematic diagram of the convexity extraction algorithm. Two digital low-pass filters (LPFs) are employed to remove the high-frequency noise existed in the measured BGS. Two-order derivative of the filtered BGS related to f is calculated to obtain the value of convexity, which is shown in Fig. 1(d). It can be observed that the trapezoidal noise structure is suppressed, leading to a potentially unlimited strain/temperature range for BOCDA.

In a BOCDA system, the nominal spatial resolution is defined as the detectable length when the signal level is equal to the noise level, which can be given as [32]

$$\Delta z=\frac{v_g\Delta v}{2\pi f_m\Delta f} \tag{5}$$

When the stretched/heated length becomes shorter than the nominal spatial resolution, the noise level will become higher than the signal level. For this case, the BFS cannot be extracted correctly with the conventional method. By using the proposed method, the Brillouin signal generated at the correlation peak is amplified while the background noise is suppressed. This means that the events with interaction length shorter than the nominal spatial resolution can be detected.

In order to verify this, simulation results of BOCDA output along a fiber which is stretched with different lengths are given. The modulation parameters f_m and Δf are set to be 2.1 MHz and 5.1 GHz, corresponding to a measurement range of 50 m and a spatial resolution of 10 cm. A 200-MHz frequency shift is assigned along the FUT with different lengths of 15 cm, 11 cm, 7 cm, 5 cm, 4 cm, 3 cm, 2.5 cm, 2 cm, 1.5 cm. Figure 2(a) and 2(b) show the Brillouin signal without and with using convexity extraction algorithm. The overall suppression of noise structure can be observed clearly in Fig. 2(b). Figure 2(c) shows the BGS (blue line) and its convexity (red line) at 1.53 m where a 5-cm-long section is assigned with a frequency shift of 200 MHz. After using convexity extraction algorithm, the SNR is improved from 0.8 to 1.7. The distributions of BFSs along the FUT extracted by the conventional method (blue line) and the proposed method (red line) are shown in Fig.2 (d). The 11-cm-long BFS-shifted section can be measured correctly using the conventional method while detection of 7-cm-long section fails since the nominal spatial resolution is a longer one of 10 cm. The red line in Fig. 2(d) shows the BFS obtained by searching for the frequency corresponding to the maximum convexity degree. The 2-cm-long section with 200-MHz frequency shift can

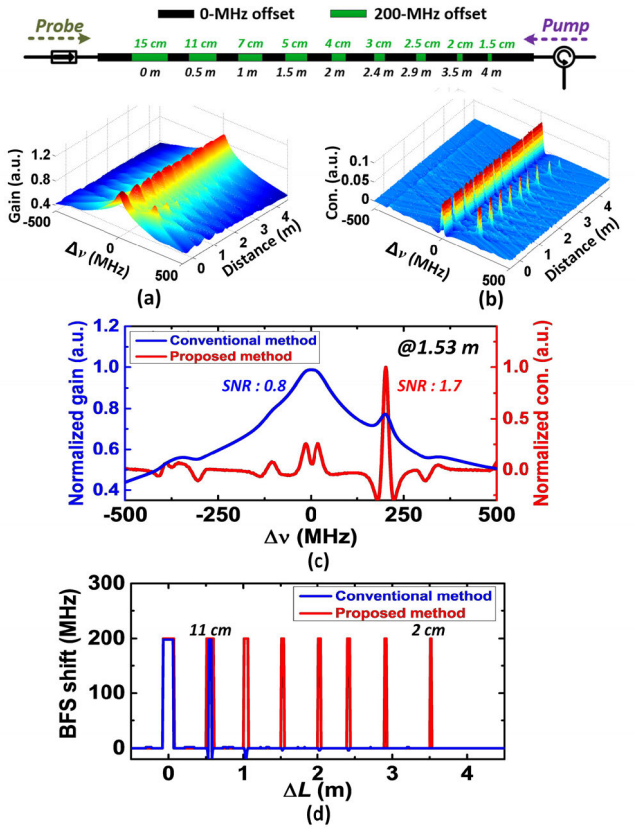

FIGURE 2. (a) Simulation result of BGS distribution along the FUT where short sections with different lengths are assigned with a Brillouin frequency shift (BFS) change of 200 MHz. (b) The convexity calculated from (a), where an overall suppression of the background noise structure can be clearly observed. (c) The BGS (blue line) and its convexity (red line) at 1.53 m where a 5-cm-long section is frequencyshifted. (d) The BFS distribution along the FUT when the conventional method (blue line) and the proposed method (red line) are utilized. A fivefold enhancement of spatial resolution is achieved when the convexity rather than the Brillouin gain is used to extract the BFS.

be measured correctly, showing a fivefold improvement of spatial resolution by using the proposed method.

III. EXPERIMENTAL SETUP AND RESULTS

The experimental setup of the BOCDA system is depicted in Fig. 3. A distributed feedback laser diode (DFB-LD, NEL, NLK1C5EAAA) with central wavelength of 1551 nm and 2-MHz linewidth is used as the light source where a sinusoidal frequency modulation is applied to synthesize periodical correlation peaks. The output of the DFB-LD is divided into two beams by a 3-dB optical coupler (OC). One beam is injected into a single-sideband modulator (SSBM) to generate the probe lightwave. The SSBM is driven by a radio-frequency (RF) signal with a frequency of ∼11 GHz which is generated using a voltage-controlled oscillator (VCO). To improve the long-term stability of the system, a servo module is introduced to stabilize the operating point of the SSBM, enabling a high sideband suppression ration (SBSR) of >25 dB. Then, an erbium-doped fiber amplifier (EDFA) is used to compensate the insertion loss induced by the SSBM.

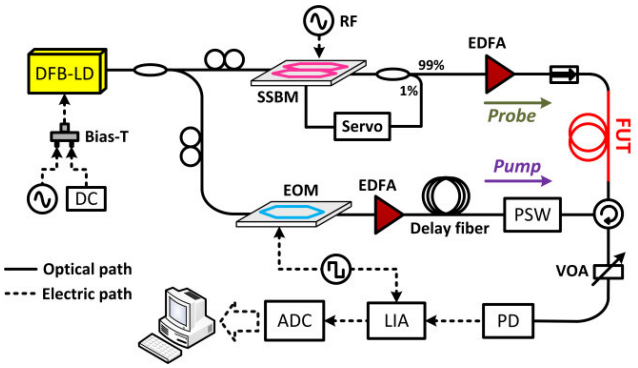

FIGURE 3. Detailed experimental setup of the BOCDA system. DFB-LD: distributed feedback laser diode; SSBM: single-sideband modulator; EDFA: erbium-doped fiber amplifier; FUT: fiber under test; EOM: electro-optic modulator; PSW: polarization switch; VOA: variable attenuator; PD: photodetector; LIA: lock-in amplifier; ADC: analog-to-digital converter.

Another beam is directly used as the pump lightwave, and another EDFA is used to improve its power to ∼23 dBm. A delay fiber is inserted into the system to locate the high-order correlation peak within the FUT. In order to mitigate the polarization-dependent gain fluctuation, a polarization switch (PSW) is inserted after the delay fiber, in which two orthogonal polarization states are alternatively applied to the pump lightwave. A 15-MHz photodiode (PD) is used as the detector to convert the optical signal to the electrical signal. In order to improve the measurement accuracy of the system, a lock-in amplification (LIA) scheme is introduced, where the pump lightwave is chopped by using an electro-optic modulator (EOM). Then the electrical signal after the LIA is acquired using a high-performance analog-to-digital converter (ADC) with a sampling rate of 15 MS/s and a resolution of 16 bit.

A. VALIDATION OF ENLARGED STRAIN OR TEMPERATURE MEASUREMENT RANGE

Firstly, the performance enhancement in strain/temperature measurement range is experimentally verified. The modulation frequency f_m and amplitude Δf of the DFB-LD are set to be 1 MHz and ∼11 GHz respectively, corresponding to a measurement range of 100 m and a spatial resolution of ∼10 cm. A 100-m single-mode fiber (SMF) is used as the FUT, where an 11-cm-long section is stretched with different strains. The modulation frequency f_m is adjusted properly to locate the correlation peak (sensing position) within the stretched section. The BGS is obtained by sweeping the output frequency of the VCO around the BFS of the FUT. The measured BGS is shown in Fig. 4 (a). It can be clearly observed that the Brillouin signal from the correlation peak shifts to a higher frequency when the strain increases, while the background noise structure remains unchanged. When the BFS change induced by the strain is larger than the maximum measurement range (∼240 MHz) of the conventional BOCDA system, the noise level becomes higher than the signal level, thus the strain information cannot be obtained correctly by using the conventional method.

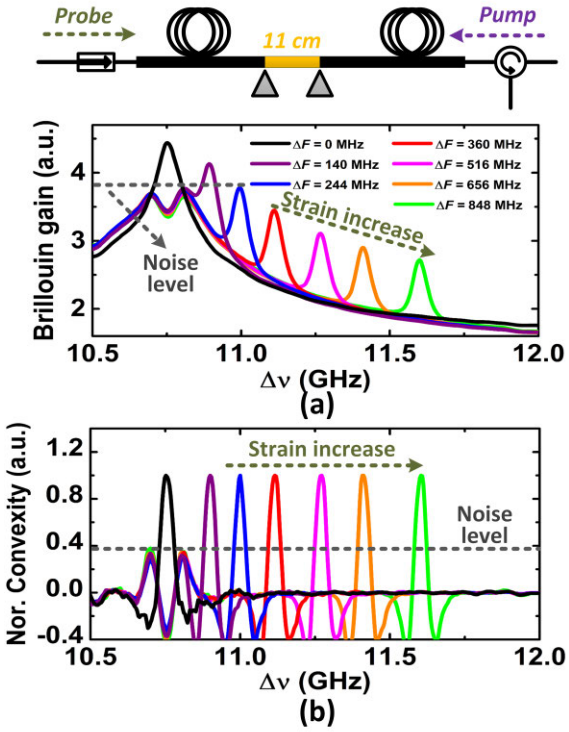

FIGURE 4. (a) Measured BGS and (b) its convexity when different strains are applied to the FUT.

As analyzed before, the Brillouin signal shows a Lorentzian shape, while the background noise structure shows a trapezoidal shape. To suppress the background noise, we calculate the convexity of the measured BGS, and the results are shown in Fig. 4(b). It can be observed that the background noise is suppressed drastically. Even though the strain-induced BFS change increases to over 800 MHz, the strain information can still be measured correctly by using the proposed method. Actually, when the convexity rather than the Brillouin gain is utilized, the strain/temperature measurement range is solely limited by the sweeping range of the VCO, which can be wider than 1 GHz easily.

B. MEASUREMENTS WITH CENTIMETER-ORDER SPATIAL RESOLUTION

Benefiting from the suppression of background noise, the events with interaction length shorter than nominal spatial resolution can be detected. To verify this, distributed measurements are implemented. Here, the modulation frequency f_m and amplitude Δf are set to be 144 kHz and ~20 GHz respectively, corresponding to a measurement range of 700 m and a spatial resolution of ~40 cm. The FUT is prepared by concatenating SMF and 4 pieces of dispersion-shifted fibers (DSFs) with lengths of 40 cm, 20 cm, 10 cm, and 8 cm. The BFSs of the SMF and the DSF are about 10.85 GHz and 10.63 GHz. By changing the modulation frequency f_m, the correlation peak is scanned along the whole FUT, thus the BGS distribution map can be obtained. Figure 5(a) shows

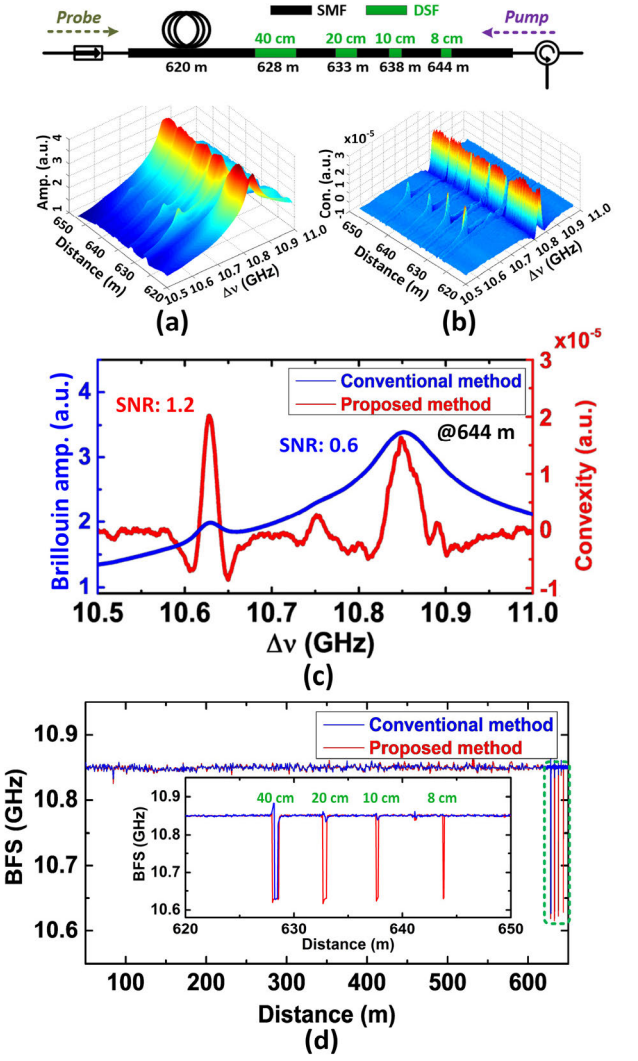

FIGURE 5. (a) Measured BGS distribution and (b) its convexity around the far end of the FUT where DSFs with different lengths are spliced. (c) Measured BGS (blue line) and its convexity (red line) at 644 m where an 8-cm-long DSF section is spliced. (d) BFS distribution along the whole FUT when the conventional method (blue line) and the proposed method (red line) are used. The modulation frequency f_m and amplitude Δf are set to be 144 kHz and ~20 GHz, respectively.

the 3-D BGS distribution around the far end of the FUT, where DSFs with different lengths are spliced. Figure 5(b) gives the convexity calculated from Fig. 5(a). An overall suppression of the noise structure can be clearly observed, leading to an improved spatial resolution. Fig. 5(c) shows the measured BGS (blue line) and its convexity (red line) at 644 m where an 8-cm-long DSF is spliced. The SNR is improved from 0.6 to 1.2 when the convexity extraction algorithm is utilized. Figure 5(d) shows the BFS distribution along the whole FUT when the conventional measuring method (blue line) and the proposed method (red line) is used, and the inset gives the detailed information around the far end of the FUT. When the Brillouin gain is used to extract the BFS, the 40-cm-long DSF section can be measured successfully,

while other DSF sections cannot be recognized. After the convexity is used instead, even the 8-cm-long DSF section can be measured accurately at a nominal spatial resolution of 40 cm, confirming an enhancing factor of five in terms of spatial resolution with the proposed method.

C. MEASUREMENTS WITH SUB-CENTIMETER SPATIAL RESOLUTION

Subsequently, we demonstrate the feasibility of the proposed method in the case of sub-cm spatial resolution. In BOCDA, the measurement range and the spatial resolution can be varied flexibly by changing the modulation parameters of the laser source. Here, the modulation frequency f_m and amplitude Δf are set to be 5.5 MHz and ∼9.5 GHz respectively, corresponding to a measurement range of 18 m and a nominal spatial resolution of ∼2 cm. The FUT is prepared by concatenating SMF and 6 pieces of DSFs with lengths of 2.2 cm, 1.5 cm, 1.1 cm, 0.7 cm, 0.5 cm, and 0.4 cm. The 3-D plot of the BGS distribution around the 0.4-cm-long DSF section is shown in Fig. 6(a). Although the Brillouin signal from the DSF can be observed (red dashed circle), the background noise stacked from other position along the FUT is very high, making it very difficult to obtain the BFS correctly. Fig. 6(b) gives the convexity of Fig. 6(a), showing an overall suppression of the noise structure. Figure 6(c) shows the measured BGS (blue line) and its convexity (red line) when the sensing position is located at the 0.4-cm-long DSF section. The SNR is improved from 0.9 to 1.5. The BFS distribution along the whole FUT is shown in Fig. 6(d). When the BFS is extracted using the Brillouin gain, the 2.2-cm-long DSF section can be measured successfully, while detection of other DSF sections fails. After the proposed method is used, benefiting from the suppression of background noise, even the 0.4-cm-long DSF can be measured, which means that the spatial resolution is improved from 2 cm to 4 mm. Here the measured BFS values of different DSF sections are not equal, which is caused by the residual strain since heat shrink tubes are used in our experiments to prevent the spliced DSF sections from breaking.

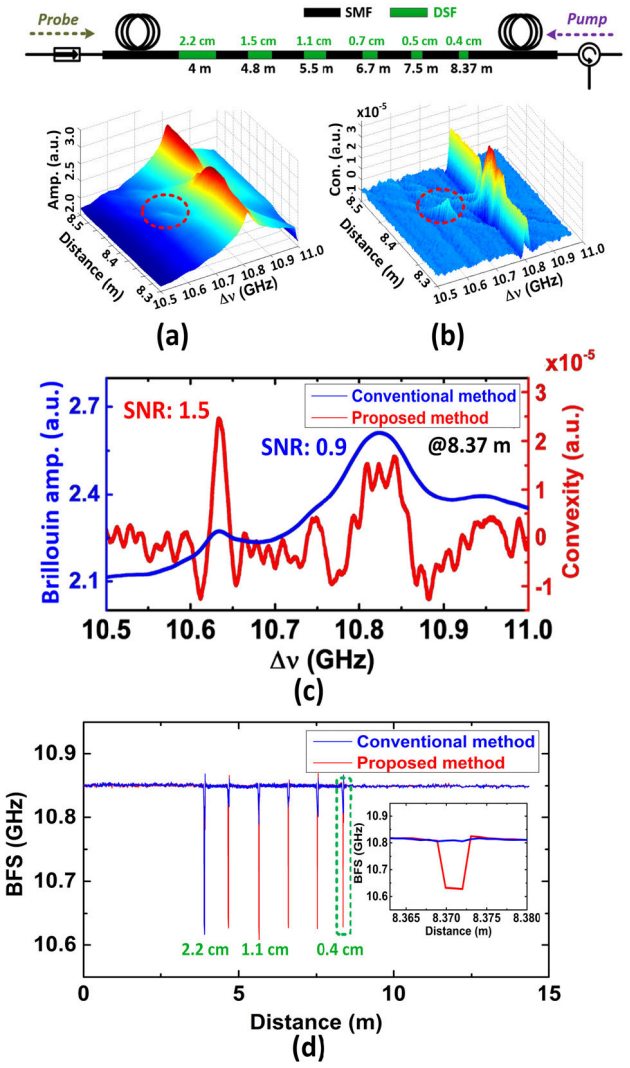

FIGURE 6. (a) Measured BGS distribution and (b) its convexity around the far end of the FUT where DSFs with different lengths are spliced. (c) Measured BGS (blue line) and its convexity (red line) at 8.37 m where a 0.4-cm-long DSF section is spliced. (d) BFS distribution along the whole FUT when the conventional method (blue line) and the proposed method (red line) are used. The modulation frequency f_m and amplitude Δf are set to be 5.5 MHz and ∼9.5 GHz, respectively.

D. DYNAMIC STRAIN MEASUREMENT

Finally, we validate the performance enhancement of the proposed system in dynamic BOCDA system. Fig. 7 shows the detailed experimental setup of dynamic BOCDA system. In conventional BOCDA system, a LIA along with a chopping configuration is employed to improve the measurement accuracy or stability. However, the measurement speed is normally less than 100 points/s due to the limited working bandwidth of the LIA. To achieve dynamic measurements, an injection-locking scheme along with a balanced detection method is introduced [26], thus removing the limitation induced by LIA. A polarization-maintaining fiber (PMF) is used as the FUT to avoid the polarization-dependent gain fluctuation. Here, a sampling rate of 1250 points/s is realized. Dynamic strains (sinusoidal shape) with frequencies up to 200 Hz are applied to a 15-cm-long section by using an electrical motor. The correlation peak is located at the stretched section, and the nominal spatial resolution is set to be ∼40 cm.

Figure 8(a) and (b) show the measured BGS within a duration of 80 ms when dynamic strains with frequencies of 50 Hz and 200 Hz are applied. It can be observed that the background noise is much higher than the Brillouin signal (red dashed circle) since the stretched length (∼15 cm) is shorter than the nominal spatial resolution (∼40 cm). Fig. 8(c) and (d) show the convexity signal calculated from (a) and (b). Benefiting from the suppression of background noise, the useful Brillouin signal (red dashed circle) can be measured with a high SNR. Fig. 9(a) and (b) show the BFS variations extracted from Fig. 8(a) and (b) when conventional method is utilized. It can be observed that the strain information

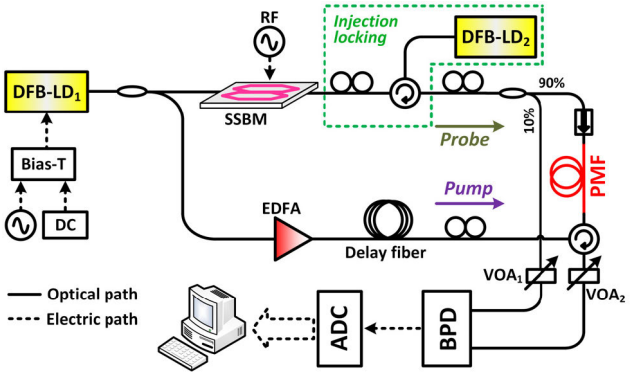

FIGURE 7. Detailed experimental setup of dynamic BOCDA system. DFB-LD: distributed feedback laser diode; SSBM: single-sideband modulator; EDFA: erbium-doped fiber amplifier; PMF: polarization-maintaining fiber; VOA: variable attenuator; BPD: balanced photodetector; LIA: lock-in amplifier; ADC: analog-to-digital converter.

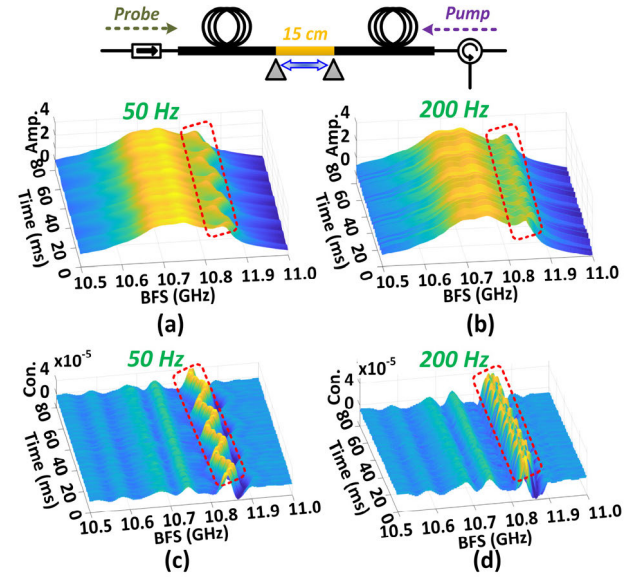

FIGURE 8. Measured BGSs at stretched section when dynamic strains with frequencies of (a) 50 Hz and (b) 200 Hz are applied. (c) and (d) are the convexity signal calculated from (a) and (b), showing a clear suppression of background noise.

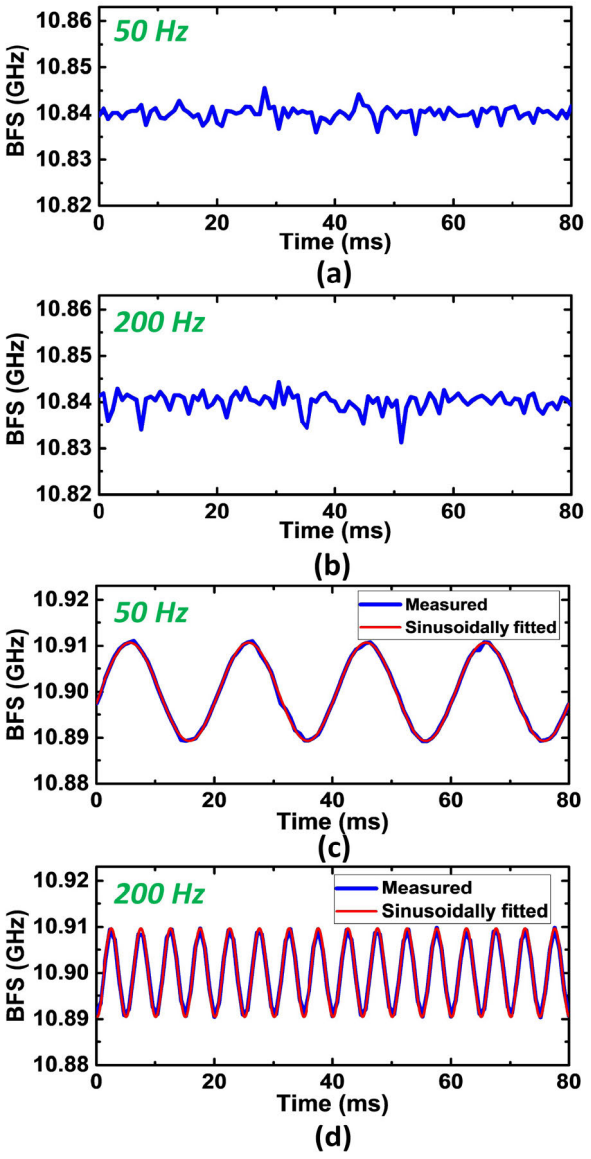

FIGURE 9. BFS variations extracted by using the conventional method ((a) and (b)) and the proposed method ((c) and (d)) when 50-Hz and 200-Hz dynamic strains are applied to the FUT.

cannot be detected correctly. Fig. 9(c) and (d) show the BFS variations obtained from Fig. 8(c) and (d) where convexity extraction algorithm is introduced. The sinusoidal dynamic strains can be measured correctly, and the period matches well with the theoretical value, verifying the enhancement of spatial resolution in dynamic BOCDA system.

IV. DISCUSSIONS

In order to remove the background noise in BOCDA, several methods have been proposed. In [30], an extra IM is inserted into the system to shape the optical spectrum of the laser source, so as to improve the SNR of the measured BGS. In this scheme, the modulation signal injected into the IM requires to be elaborately designed to optimize the performance of this technique. Alternately, a differential detection scheme is demonstrated by utilizing a phase modulator (PM) to chop the pump wave [31]. In these two schemes, a rigid synchronization between the signal applied to the IM (or the PM) and the modulation signal of the laser source is required, which not only increases the complexity for instrument control but also makes them unsuitable for dynamic measurements. In [34], a noise-floor compensation method with capability of removing the background noise has been proposed. However, this method cannot work properly under some extreme measurement conditions, for example when large strain is applied to the fiber. On the contrary, the data-processing method reported in this paper is capable of suppressing the background noise without extra hardware complexity, and it can be used in various measurement conditions.

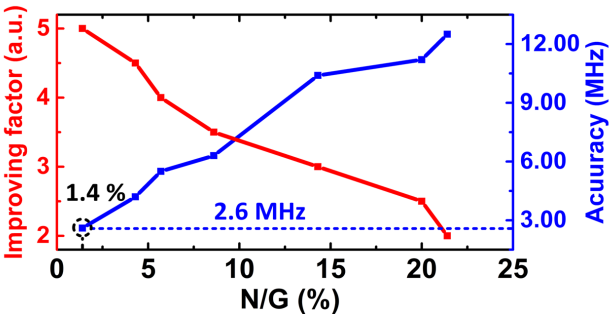

FIGURE 10. The improving factor of spatial resolution (red-dotted line) and the measurement accuracy (blue-dotted line) at different noise-to-gain ratio (N/G).

As for all Brillouin correlation-domain sensors, including sinusoidal-modulation-based BOCDA [3], chaotic BOCDA [19], and Brillouin optical correlation domain reflectometry (BOCDR) [35], distributed measurements are all achieved by synthesizing sharp correlation peaks. Therefore, the proposed method can also be used in these correlation-domain systems to improve their performance. In some cases, especially in high-speed BOCDA system, the measured BGS is not very smooth, which may deteriorate the performance of the proposed technique. Here we discuss the effect of the high-frequency noise by simulation. The noisy BGS can be expressed as

$$G_N(x,f) = G(x,f) + N(x,f) \tag{6}$$

where $N(x,f)$ is the white noise added on the BGS. In the proposed convexity extraction algorithm, low-pass filters are utilized to remove the high-frequency noise from the BGS. The simulation results are shown in Fig. 10. We define the improving factor as the ratio between the nominal spatial resolution and the shortest detectable length achieved by the proposed technique. It can be clearly observed that when the noise level increases, the improving factor is decreased and the measurement accuracy is deteriorated, as shown in Fig. 10. It is desired to notification that, for most Brillouin correlation-domain sensing systems, the noise-to-gain ratio (N/G) is lower than 1.4% (or the measurement accuracy is better than 2.6 MHz). Thus, an improving factor of five can be achieved for most Brillouin correlation-domain sensors. When the N/G increases to 5.7%, the measurement accuracy is deteriorated to be 5.5 MHz accordingly. In this case, the improving factor is decreased to four.

V. CONCLUSION

In this paper, we propose and experimentally demonstrate a novel method to improve the strain/temperature measurement range and the spatial resolution of the BOCDA system by exploiting the convexity of the measured BGS. By analyzing the shape feature of the Brillouin signal from the correlation peak and the background noise structure accumulated from other positions, we found that the Brillouin signal has a high value of convexity while the noise structure has a low value of convexity. Therefore, by calculating the convexity of the measured BGS, the trapezoidal-shape noise structure can be suppressed drastically, which leads to an enlarged strain/temperature measurement range and a narrowed spatial resolution. The feasibility of the proposed method is verified by both numerical simulation and experiments. A potentially unlimited strain/temperature measurement range as well as a fivefold-enhanced spatial resolution is obtained without extra hardware complexity. Although the concept is only demonstrated in the BOCDA system based on sinusoidal frequency modulation, we believe that the proposed method can also be used in other correlation-domain systems including chaotic BOCDA, BOCDR, and correlation-domain Brillouin dynamic grating (BDG)-based sensors.

REFERENCES

[1] T. Kurashima, T. Horiguchi, H. Izumita, S. I. Furukawa, and Y. Koyamada, "Brillouin optical-fiber time domain reflectometry," *IEICE Trans. Commun.*, vol. E76-B, pp. 382–390, Apr. 1993.
[2] D. Garus, K. Krebber, F. Schliep, and T. Gogolla, "Distributed sensing technique based on Brillouin optical-fiber frequency-domain analysis," *Opt. Lett.*, vol. 21, no. 17, pp. 1402–1404, Sep. 1996.
[3] K. Hotate, "Measurement of Brillouin gain spectrum distribution along an optical fiber using a correlation-based technique–proposal, experiment and simulation," *IEICE Trans. Electron.*, vol. E83-C, no. 3, pp. 405–412, Mar. 2000.
[4] Y. Dong, L. Chen, and X. Bao, "Time-division multiplexing-based BOTDA over 100 km sensing length," *Opt. Lett.*, vol. 36, no. 2, pp. 277–279, 2011.
[5] X. Angulo-Vinuesa *et al.*, "Raman-assisted brillouin distributed temperature sensor over 100 km featuring 2 m resolution and 1.2°C uncertainty," *J. Lightw. Technol.*, vol. 30, no. 8, pp. 1060–1065, Apr. 15, 2012.
[6] M. A. Soto, G. Bolognini, and F. Di Pasquale, "Long-range simplex-coded BOTDA sensor over 120 km distance employing optical preamplification," *Opt. Lett.*, vol. 36, no. 2, pp. 232–234, 2011.
[7] M. A. Soto, S. Le Floch, and L. Thévenaz, "Bipolar optical pulse coding for performance enhancement in BOTDA sensors," *Opt. Express*, vol. 21, no. 14, pp. 16390–16397, Jul. 2013.
[8] W. Li, X. Bao, Y. Li, and L. Chen, "Differential pulse-width pair BOTDA for high spatial resolution sensing," *Opt. Express*, vol. 16, no. 26, pp. 21616–21625, 2008.
[9] Y. Dong, X. Bao, and W. Li, "Differential Brillouin gain for improving the temperature accuracy and spatial resolution in a long-distance distributed fiber sensor," *Appl. Opt.*, vol. 48, no. 22, pp. 4297–4301, Aug. 2009.
[10] Y. Dong, H. Zhang, L. Chen, and X. Bao, "2 cm spatial-resolution and 2 km range Brillouin optical fiber sensor using a transient differential pulse pair," *Appl. Opt.*, vol. 51, no. 9, pp. 1229–1235, Mar. 2012.
[11] S. Foaleng-Mafang, J.-C. Beugnot, and L. Thévenaz, "Optimized configuration for high resolution distributed sensing using Brillouin echoes," *Proc. SPIE*, vol. 7503, Oct. 2009, Art. no. 75032C.
[12] S. M. Foaleng, M. Tur, J.-C. Beugnot, and L. Thévenaz, "High spatial and spectral resolution long-range sensing using Brillouin echoes," *J. Lightw. Technol.*, vol. 28, no. 20, pp. 2993–3003, Oct. 15, 2010.
[13] A. W. Brown, B. G. Colpitts, and K. Brown, "Dark-pulse brillouin optical time-domain sensor with 20-mm spatial resolution," *J. Lightw. Technol.*, vol. 25, no. 1, pp. 381–386, Jan. 2007.
[14] A. Zadok, Y. Antman, N. Primerov, A. Denisov, J. Sancho, and L. Thévenaz, "Random-access distributed fiber sensing," *Laser Photon. Rev.*, vol. 6, no. 5, pp. L1–L5, Sep. 2012.
[15] A. Denisov, M. A. Soto, and L. Thévenaz, "Going beyond 1000000 resolved points in a Brillouin distributed fiber sensor: Theoretical analysis and experimental demonstration," *Light Sci. Appl.*, vol. 5, no. 5, May 2016, Art. no. e16074.
[16] R. Cohen, Y. London, Y. Antman, and A. Zadok, "Few millimeter-resolution Brillouin optical correlation domain analysis using amplified-spontaneous-emission pump and signal waves," *Proc. SPIE*, vol. 9157, Jun. 2014, Art. no. 91576B.
[17] R. Cohen, Y. London, Y. Antman, and A. Zadok, "Brillouin optical correlation domain analysis with 4 millimeter resolution based on amplified spontaneous emission," *Opt. Express*, vol. 22, no. 10, pp. 12070–12078, May 2014.

[18] J. Zhang, C. Feng, M. Zhang, Y. Liu, C. Wu, and Y. Wang, "Brillouin optical correlation domain analysis based on chaotic laser with suppressed time delay signature," *Opt. Express*, vol. 26, no. 6, pp. 6962–6972, Mar. 2018.
[19] J. Z. Zhang *et al.*, "Chaotic Brillouin optical correlation domain analysis," *Opt. Lett.*, vol. 43, no. 8, pp. 1722–1725, Apr. 2018.
[20] K. Y. Song, Z. He, and K. Hotate, "Distributed strain measurement with millimeter-order spatial resolution based on Brillouin optical correlation domain analysis," *Opt. Lett.*, vol. 31, no. 17, pp. 2526–2528, Sep. 2006.
[21] K. Y. Song and K. Hotate, "Distributed fiber strain sensor With 1-kHz sampling rate based on Brillouin optical correlation domain analysis," *IEEE Photon. Technol. Lett.*, vol. 19, no. 23, pp. 1928–1930, Dec. 1, 2007.
[22] K. Y. Song, M. Kishi, Z. He, and K. Hotate, "High-repetition-rate distributed Brillouin sensor based on optical correlation-domain analysis with differential frequency modulation," *Opt. Lett.*, vol. 36, no. 11, pp. 2062–2064, Jun. 2011.
[23] C. Zhang, M. Kishi, and K. Hotate, "5,000 points/s high-speed random accessibility for dynamic strain measurement at arbitrary multiple points along a fiber by Brillouin optical correlation domain analysis," *Appl. Phys. Express*, vol. 8, no. 4, Mar. 2015, Art. no. 042501.
[24] B. Wang, X. Fan, J. Du, and Z. He, "Performance enhancement of Brillouin optical correlation domain analysis based on frequency chirp magnification," *Chin. Opt. Lett.*, vol. 15, no. 12, Dec. 2017, Art. no. 120601.
[25] B. Wang, X. Fan, Q. Liu, and Z. He, "Increasing effective sensing points of Brillouin optical correlation domain analysis using four-wave-mixing process," *Proc. SPIE*, vol. 10323, Apr. 2017, Art. no. 103238K.
[26] B. Wang, X. Fan, Y. Fu, and Z. He, "Dynamic strain measurement with kHz-level repetition rate and centimeter-level spatial resolution based on Brillouin optical correlation domain analysis," *Opt. Express*, vol. 26, no. 6, pp. 6916–6928, Mar. 2018.
[27] K. Hotate and H. Arai, "Enlargement of measurement range of simplified BOCDA fiber-optic distributed strain sensing system using a temporal gating scheme," *Proc. SPIE*, vol. 5855, pp. 184–187, May 2005.
[28] W. Zou, Z. He, and K. Hotate, "Range elongation of distributed discrimination of strain and temperature in Brillouin optical correlation-domain analysis based on dual frequency modulations," *IEEE Sensors J.*, vol. 14, no. 1, pp. 244–248, Jan. 2014.
[29] J. H. Jeong, K. Lee, K. Y. Song, J.-M. Jeong, and S. B. Lee, "Bidirectional measurement for Brillouin optical correlation domain analysis," *Opt. Express*, vol. 20, no. 10, pp. 11091–11096, Apr. 2012.
[30] K. Y. Song, Z. He, and K. Hotate, "Effects of Intensity Modulation of Light Source on Brillouin Optical Correlation Domain Analysis," *J. Lightw. Technol.*, vol. 25, no. 5, pp. 1238–1246, May 2007.
[31] J. H. Jeong, K. Lee, K. Y. Song, J.-M. Jeong, and S. B. Lee, "Differential measurement scheme for Brillouin optical correlation domain analysis," *Opt. Express*, vol. 20, no. 24, pp. 27094–27101, Dec. 2012.
[32] T. Yamauchi and K. Hotate, "Performance evaluation of Brillouin optical correlation domain analysis for fiber optic distributed strain sensing by numerical simulation," *Proc. SPIE*, vol. 5589, pp. 164–173, Dec. 2004.
[33] A. Kobyakov, M. Sauer, and D. Chowdhury, "Stimulated Brillouin scattering in optical fibers," *Adv. Opt. Photon.*, vol. 2, no. 1, pp. 1–59, Mar. 2010.
[34] Y. Mizuno, Z. He, and K. Hotate, "Stable entire-length measurement of fiber strain distribution by Brillouin optical correlation-domain reflectometry with polarization scrambling and noise-floor compensation," *Appl. Phys. Express*, vol. 2, no. 6, 2009, Art. no. 062403.
[35] Y. Mizuno, W. Zou, Z. He, and K. Hotate, "Proposal of Brillouin optical correlation-domain reflectometry (BOCDR)," *Opt. Express*, vol. 16, no. 16, pp. 12148–12153, Jul. 2008.

BIN WANG was born in Hunan, China, in 1992. He received the B.S. degree in communication engineering from the Huazhong University of Science and Technology, Wuhan, China, in 2014. He is currently pursuing the Ph.D. degree with Shanghai Jiao Tong University, Shanghai, China. His research interests include distributed fiber-optic sensing and microwave photonics.

XINYU FAN (M'06–SM'18) was born in Jiangsu, China, in 1978. He received the B.S. and M.S. degrees in applied physics from Shanghai Jiao Tong University, Shanghai, China, in 2000 and 2003, respectively, and the Ph.D. degree in electrical engineering from The University of Tokyo, Tokyo, Japan, in 2006. In 2006, he joined NTT Access Network Service Systems Laboratories, Japan, where his research interests include optical reflectometry and optical measurement. Since 2012, he has been with the Department of Electrical Engineering, Shanghai Jiao Tong University, where he is currently a Professor. His research interests include optical fiber sensing technology, optical fiber measurement, and fiber-related applications. He is a Senior Member of the Optical Society of America.

YUANXIU FU was born in Zhejiang, China, in 1994. He received the B.S. degree in electronic science and technology from the Shanghai Jiao Tong University, Shanghai, China, in 2017, where he is currently pursuing the M.S. degree. His research interest includes distributed fiber-optic sensing.

ZUYUAN HE (M'00–SM'11) received the B.S. and M.S. degrees in electronic engineering from Shanghai Jiao Tong University, Shanghai, China, in 1984 and 1987, respectively, and the Ph.D. degree in optoelectronics from the University of Tokyo, Tokyo, Japan, in 1999. He joined the Nanjing University of Science and Technology, Nanjing, China, as a Research Associate, in 1987, and became a Lecturer in 1990. From 1995 to 1996, he was a Research Fellow studying optical information processing with the Research Center for Advanced Science and Technology, University of Tokyo. In 1999, he became a Research Associate with the University of Tokyo, where he worked on the measurement and characterization of fiber optic components and systems, fiber optic reflectometry, fiber optic sensors, and multidimensional optical information processing. In 2001, he joined CIENA Corporation, Linthicum, MD, USA, as a Lead Engineer, leading the Optical Testing and Optical Process Development Group. He returned to the University of Tokyo as a Lecturer, in 2003, and became an Associate Professor, in 2005, and the Full Professor, in 2010. He is currently a Chair Professor and the Director of the State Key Laboratory of Advanced Optical Communication Systems and Networks, Shanghai Jiao Tong University, Shanghai, China. His current research interests include optical fiber sensors, specialty optical fibers, and optical interconnection. He is a Senior Member of the Optical Society of America and a member of the Institute of Electronics, Information, and Communication Engineers of Japan.